Sporopollenin Biosynthetic Enzymes Interact and Constitute a Metabolon Localized to the Endoplasmic Reticulum of Tapetum Cells[W]

Benjamin Lallemand, Mathieu Erhardt, Thierry Heitz, and Michel Legrand*

Institut de Biologie Moléculaire des Plantes, Unité Propre de Recherche 2357 du Centre National de la Recherche Scientifique, Université de Strasbourg, 67084 Strasbourg cedex, France

The sporopollenin polymer is the major constituent of exine, the outer pollen wall. Recently fatty acid derivatives have been shown to be the precursors of sporopollenin building units. ACYL-COA SYNTHETASE, POLYKETIDE SYNTHASE A (PKSA) and PKSB, TETRAKETIDE α-PYRONE REDUCTASE1 (TKPR1) and TKPR2 have been demonstrated to be involved in sporopollenin biosynthesis in Arabidopsis (*Arabidopsis thaliana*). Here all these sporopollenin biosynthetic enzymes but TKPR2 have been immunolocalized to endoplasmic reticulum of anther tapetal cells. Pull-down experiments demonstrated that tagged recombinant proteins interacted to form complexes whose constituents were characterized by immunoblotting. In vivo protein interactions were evidenced by yeast (*Saccharomyces cerevisiae*) two-hybrid analysis and by fluorescence lifetime imaging microscopy/Förster resonance energy transfer studies in transgenic *Nicotiana benthamiana*, which were used to test the possibility that the enzymes interact to form a biosynthetic metabolon. Various pairs of proteins fused to two distinct fluorochromes were coexpressed in *N. benthamiana* leaf tissues and fluorescence lifetime imaging microscopy/Förster resonance energy transfer measurements demonstrated that proteins interacted pairwise in planta. Taken together, these results suggest the existence of a sporopollenin metabolon.

Anthers of angiosperm flowers produce the male microsporocytes that undergo meiosis and give rise to tetrads of four haploid microspores. During anther development, the microspores develop into pollen grains relying on both sporophytic and gametophytic gene functions (Owen and Makaroff, 1995; Scott et al., 2004; Blackmore et al., 2007). Cellulosic primexine and pectocellulosic intine are synthesized by the microspores and constitute the inner layers of the pollen wall. The tapetum, the innermost cell layer of the anther locule, supplies nutrients, structural components, and enzymes necessary to build up the outer layer of the pollen wall called exine. The main constituent of exine is the sporopollenin polymer, whose precursors are secreted into the anther locule and deposited on microspores to form the sculptured baculae and tecta of the exine. Sporopollenin is a chemically inert biopolymer that is insoluble in both aqueous and organic solvents and whose resistance to nonoxidative degradation has been a hindrance to the determination of its exact structure. Analytical methods have, however, revealed that sporopollenin is mainly composed of long, polyhydroxylated aliphatic chains and of small amounts of aromatic rings derived from the phenylpropanoid metabolism (Dominguez et al., 1999; Bubert et al., 2002; Ahlers et al., 2003).

Recently, the isolation and analysis of numerous Arabidopsis (*Arabidopsis thaliana*) mutants exhibiting defects in exine structure have demonstrated that a large array of sporophytic genes are involved in tapetum development and exine formation (Aarts et al., 1997; Paxson-Sowders et al., 2001; Morant et al., 2007; Suzuki et al., 2008; de Azevedo Souza et al., 2009; Dobritsa et al., 2009a, 2009b, 2010, 2011; Tang et al., 2009; Grienenberger et al., 2010; Ishiguro et al., 2010; Kim et al., 2010; Quilichini et al., 2010; Ariizumi and Toriyama, 2011; Chen et al., 2011b; Choi et al., 2011; Dou et al., 2011). These genes encode distinct classes of products such as transcription regulators or enzymes or structural components, thus illustrating the complexity of the processes involved in pollen development (Ariizumi and Toriyama, 2011). However, only in a few cases has the exact gene function in pollen development been identified. Two cytochromes P450s (CYP450s) have been demonstrated to catalyze in-chain hydroxylation or ω-hydroxylation of medium- and long-chain fatty acids (Morant et al., 2007; Dobritsa et al., 2009b). Fatty acids activated by ACYL-COA SYNTHETASE5 (ACOS5) give rise to fatty acyl-CoA esters (de Azevedo Souza et al., 2009). CoA esters are condensed to malonyl-CoA by polyketide synthases PKSA and PKSB yielding tri- and tetraketide α-pyrone products (Mizuuchi et al., 2008; Dobritsa et al., 2010; Kim et al., 2010). The resulting tetraketide products are then reduced by tetraketide reductases

* Corresponding author; e-mail michel.legrand@ibmp-cnrs.unistra.fr.

The author responsible for distribution of materials integral to the findings presented in this article in accordance with the policy described in the Instructions for Authors (www.plantphysiol.org) is: Thierry Heitz (thierry.heitz@ibmp-cnrs.unistra.fr).

[W] The online version of this article contains Web-only data.

www.plantphysiol.org/cgi/doi/10.1104/pp.112.213124

TKPR1 and TKPR2 (Grienenberger et al., 2010). The *Male Sterile2* gene, also required for exine formation, encodes a fatty acyl-carrier protein reductase that produces fatty alcohols (Chen et al., 2011b). The polyhydroxyalkyl α-pyrone monomers together with the fatty acids and fatty alcohols are prone to form ether or ester linkages, contributing to the strong chemical and physical resistance of the sporopollenin polymer. Phylogenetic studies have shown that the genes involved in sporopollenin biosynthesis are conserved from the moss *Physcomitrella patens* to gymnosperm and angiosperm species, thus suggesting that they participate in an ancient, conserved metabolic pathway that was probably determinant in the evolution of land plants.

The sites of synthesis and transport of sporopollenin precursors in tapetal cells, as well as the mechanisms of secretion of sporopollenin monomers to the extracellular locules before polymerization in the microspore walls, are not known. In Arabidopsis anther, secretion into the locule may involve the ATP-binding cassette (ABC) transporter ABCG26/WBC27 (Quilichini et al., 2010; Choi et al., 2011; Dou et al., 2011). In rice (*Oryza sativa*), lipid transfer proteins have been shown to be required for exine formation and to be secreted into the anther locule (Huang et al., 2009; Zhang et al., 2010). Plant fatty acids are synthesized de novo in the plastids and their subsequent modifications such as unsaturation, elongation, or hydroxylation take place in the endoplasmic reticulum (ER). Many ultrastructural changes that are associated with an active lipid metabolism have been reported in tapetal cells during anther development (Owen and Makaroff, 1995; Wu et al., 1997; Piffanelli et al., 1998; Zheng et al., 2003; Hsieh and Huang, 2005; Ishiguro et al., 2010). For example, the dilation and proliferation of the ER and the accumulation of numerous vesicles and tapetum-specific lipid-containing organelles, namely elaioplasts and lipid bodies (also called tapetosomes), have been observed in tapetal cells of developing anthers (Murgia et al., 1991; Owen and Makaroff, 1995; Clément et al., 1998; Zheng et al., 2003; Ishiguro et al., 2010). At a late stage of anther development the tapetum cells lyze and elaioplast and tapetosome content is discharged to the locule and deposited, at least in part, into exine cavities to form the pollen coat (Piffanelli et al., 1997, 1998; Wu et al., 1997, 1999; Hernández-Pinzón et al., 1999; Hsieh and Huang, 2005, 2007).

Here we present immunogold labeling data showing that several enzymes of the sporopollenin biosynthetic pathway, namely ACOS5, PKSA and PKSB, and TKPR1 mainly localize to the ER compartment of tapetal cells. In contrast, immunocytochemical localization of TKPR2 demonstrated that this tetraketide α-pyrone reductase is cytoplasmic. The colocalization of four sporopollenin biosynthetic enzymes to the endoplasmic reticulum prompted us to investigate the possibility that these enzymes interact physically. Tagged recombinant proteins were demonstrated to interact together in vitro by pull-down experiments and to form protein complexes in which interacting proteins were identified on western blots using specific antibodies. In vivo interactions were investigated in yeast (*Saccharomyces cerevisiae*) by two-hybrid analysis and in *Nicotiana benthamiana* transformed with various reporter constructs. When various couples of proteins labeled with two distinct fluorochromes were coexpressed in *N. benthamiana* leaf tissues, fluorescence lifetime imaging microscopy (FLIM)/Förster resonance energy transfer (FRET) experiments demonstrated that proteins interacted in planta, thus suggesting the occurrence of a sporopollenin metabolon that may explain the high efficiency of the biosynthetic pathway leading to sporopollenin monomers.

RESULTS

Several Enzymes of the Sporopollenin Pathway Localize to ER

Exine constituents are produced in the tapetum cell layer of the anthers and then are secreted into the locules. The synthesis of fatty acid precursors takes place in tapetum plastids, and fatty acids are activated with CoA by the acyl-CoA synthetase ACOS5 and transported to the cytoplasm. ACOS5, the polyketide synthases PKSA and PKSB, and the tetraketide reductases TKPR1 and TKPR2 have all been shown recently to be required for exine formation and to constitute the biosynthetic pathway leading to sporopollenin monomers (Grienenberger et al., 2010; Kim et al., 2010). Exine is formed at a rapid pace during the development of microspores into mature pollen grains that is completed in a few hours (Owen and Makaroff, 1995; Sanders et al., 1999; Scott et al., 2004; Blackmore et al., 2007; Ariizumi and Toriyama, 2011). This implies a high rate of synthesis of sporopollenin monomers and thus an efficient catalysis of products by the enzymes involved in the pathway. To understand how the pathway is regulated and organized in tapetal cells, we first immunolocalized the enzymes involved in sporopollenin biosynthesis. Closed flower buds were collected at stage 10 of flower development, as defined by Smyth et al., 1990, and contained stamens at stages 8 to 9, as defined by Sanders et al., 1999, that were shown to highly express the sporopollenin biosynthetic pathway (Grienenberger et al., 2010; Kim et al., 2010).

Specific antibodies raised against purified recombinant proteins were used to probe anther sections. Figure 1 presents the immunochemical localization of the enzymes in tapetal cells by transmission electron microscopy (TEM). As shown in Figure 1A, no significant labeling was detected in preimmune-treated control sections. Sections probed with anti-PKSA antibodies revealed a strong immunogold labeling in tapetal cells (Fig. 1B). The labeling was mainly associated with ER, which is abundant in tapetal cells, and this is particularly evident at high magnification (see

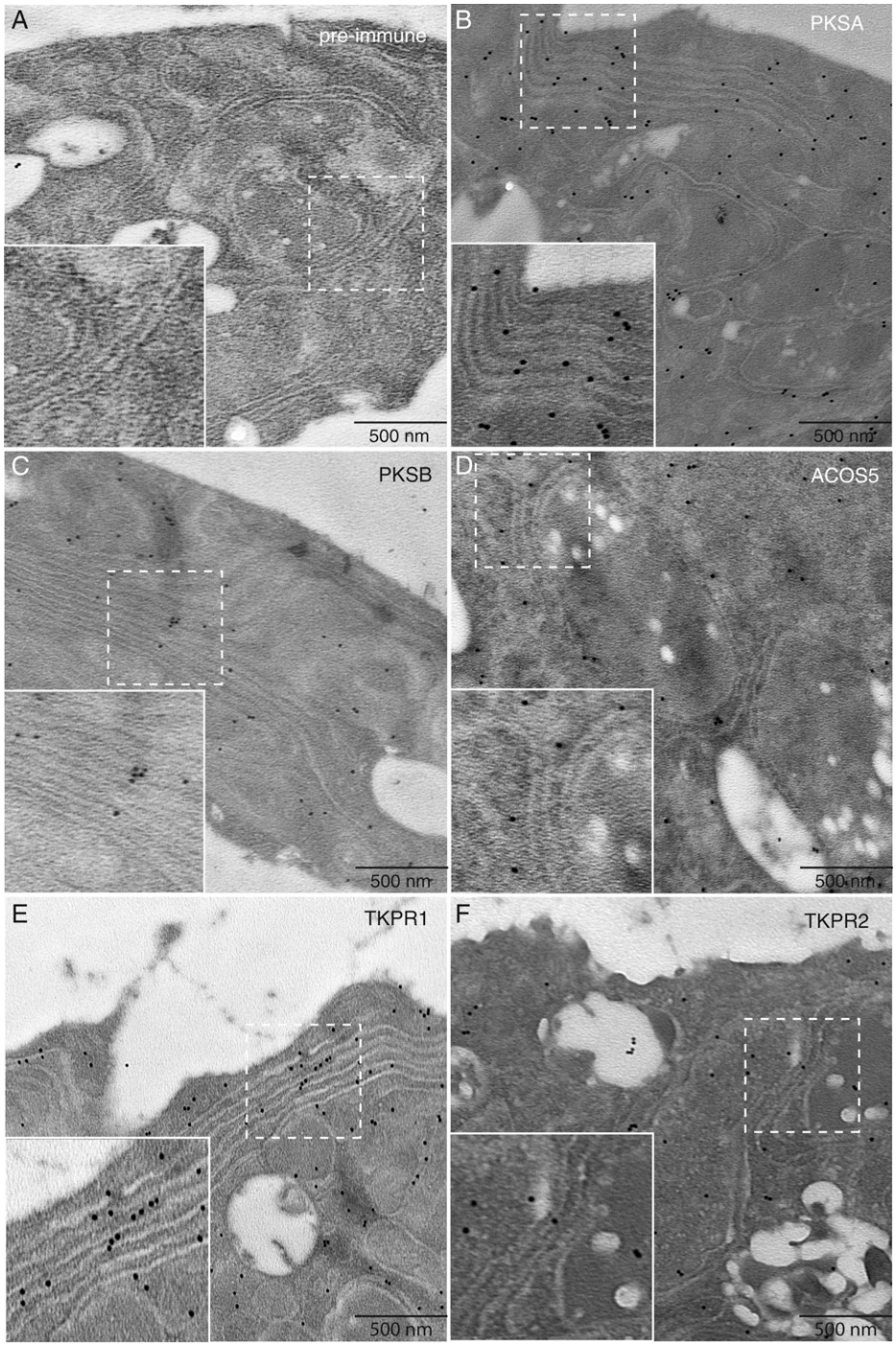

Figure 1. Immunolocalization of enzymes involved in sporopollenin pathway to the ER of tapetal cells. Anther sections were incubated with sera raised against different purified proteins of the sporopollenin pathway. A, Preimmune control serum showing no immunogold labeling. B, Immunogold labeling of PKSA was mainly localized to the ER. C, PKSB labeling also localized to the ER. D, Only a part of ACOS5 labeling was found associated with the ER compartment. E, TKPR1 immunolabeling mainly localized to the ER. F, Immunogold labeling of TKPR2 was randomly localized. The areas indicated by dotted lines are shown at higher magnification in the bottom left corners of the photographs.

insert in Fig. 1B). A similar ER localization was observed for PKSB immunogold labeling (Fig. 1C). In the case of ACOS5, the labeling was found to be associated in part with ER, but another part of the labeling was detected elsewhere in the cytoplasm (Fig. 1D). When the number of ER-associated labeling spots was quantified on numerous anther sections, distinct ratios of ER labeling to total labeling were found for the different enzymes. Table I shows that about 80% of PKSA and PKSB labeling localized to the ER compartment. On the numerous tapetal cell sections that were observed after immunolabeling, the ER compartment occupied 21% to 32% of the cell volume as measured on micrographs using the ImageJ program. Thus, the data clearly demonstrate the localization of PKS proteins on the ER. Concerning ACOS5, 50% of the labeling appeared to be associated with ER, the other 50% of the labeling spots being detected

Table I. *Quantification of immunogold signal in tapetal cells*

The number of dots on TEM micrographs were counted, and the proportion of labeling associated with ER for each protein was expressed as the percentage of the total number of dots (*n*).

Antibodies Against	Ratio of ER Labeling
	% (*n*)
ACOS5	52 (880)
PKSA	82 (4,367)
PKSB	80 (969)
TKPR1	80 (2,359)
TKPR2	35 (1,854)

elsewhere in cytoplasm (Fig. 1D; Table I). These figures are significantly higher than the ER surface ratio on micrographs (21%–32%) and indicate a preferential localization of ACOS5 to the ER, even though a part of the protein remains soluble and localizes to cytoplasm compartment. TKPR1 appeared mainly associated with ER membranes, as the majority of spots localized to the ER (Fig. 1E) in contrast to TKPR2, the labeling of which was found distributed over the whole tapetal cell without distinct localization (Fig. 1F). These observations were confirmed by the evaluation of the proportion of spots detected in the ER compartment over the total number of labeling spots. Table I shows that a large part of TKPR1 labeling (80%) was found associated with the ER similarly to what was measured for PKSA and PKSB proteins and in sharp contrast to the low ratio of ER-localized TKPR2 labeling (35%). These results indicate that the two reductases have distinct cellular localization, and this finding is in agreement with the data obtained previously by confocal microscopy (Grienenberger et al., 2010; Kim et al., 2010).

The colocalization of several sporopollenin biosynthetic enzymes on the endoplasmic reticulum of tapetal cells suggests the potential existence of protein-protein interactions that may favor the metabolic flux along the biosynthetic chain. Therefore we used various assays to test this possibility in vivo and in vitro.

Protein-Protein Interactions Evidenced by Copurification of Proteins Involved in Complexes: Pull-Down Experiments

Recombinant proteins bearing His tags were expressed in bacteria and bound to nickel-bearing affinity gel. They were used as baits and were tested for their capacity to capture candidate prey in pull-down experiments. Potential bait and prey proteins were coincubated and then passed through affinity gel, bait being immobilized on agarose beads by its His tag. After washing, proteins were eluted, and the presence of the prey in the protein complexes was tested by immunoblotting using specific antibodies. Results are presented in Figure 2. When ACOS5 was used as bait, PKSA and TKPR1 were found in protein complexes bound to the affinity beads, whereas no prey was captured in the absence of the bait, thus showing that the bait-prey interactions were specific (Fig. 2A). Similarly, when used as baits, PKSA and PKSB interacted with ACOS5 and TKPR1, which were pulled down in protein complexes bound to affinity gel (Fig. 2, B and C). Controls performed without either PKSA or PKSB as bait were negative, thus excluding the occurrence of nonspecific interaction of the prey with the affinity beads (Fig. 2, B and C). With ACOS5, PKSA, or PKSB as bait, TKPR2 was never found in protein fraction pulled down on affinity beads (Fig. 2C), revealing that, in contrast to the other reductase TKPR1, TKPR2 is not associated in complexes involving ACOS5, PKSA, and PKSB.

Interactions between Proteins Expressed in Yeast

We performed a yeast two-hybrid analysis of protein-protein interactions involving ACOS5 and the other sporopollenin biosynthetic enzymes. To that aim, we produced fusions to either the GALACTOSE4 (GAL4) DNA-binding domain (BD) or activation domain (AD). After yeast transformation with different couples of AD and BD constructs, mating mixtures were plated on yeast media lacking Leu, Trp, and His to select transformed colonies wherein protein interactions would lead to *HIS3* gene activation. This was the case when yeast was transformed with AD-PKSB and BD-ACOS5 constructs (Fig. 3B, line B/5), AD-TKPR1 and BD-ACOS5 constructs (Fig. 3B, line 1/5), and AD-CYP703 and BD-ACOS5 constructs (Fig. 3B, line 3/5), thus revealing that ACOS5 interacted with PKSB, TKPR1, and CYP703 in yeast two-hybrid assay. It is noteworthy that the reverse combinations (where the baits were used as prey and the prey as baits) did allow growth on His-depleted media only for colonies transformed with AD-ACOS5 and BD-CYP703 (Fig. 3B, line 5/3), thus indicating effective interactions between ACOS5 and CYP703 proteins in both orientations, in contrast with negative data observed with ACOS5/CYP704 proteins. Most importantly, all the controls where the bait or prey constructs were introduced in yeast together with an empty AD or BD plasmid respectively, were negative (Fig. 3B, 0/X or X/0). These negative controls demonstrated that no autoactivation of the baits or prey alone occurred and thus the growth of transformed colonies on selective media was due to protein-protein interactions between baits and prey.

FLIM/FRET Analysis Showed the Close Proximity of the Enzymes on the ER in Planta

We used FRET measured by FLIM to investigate the occurrence of protein interactions in transgenic *N. benthamiana* leaves. FRET is the process by which energy absorbed by one fluorescent protein, the donor, is transferred to another fluorescent protein, the

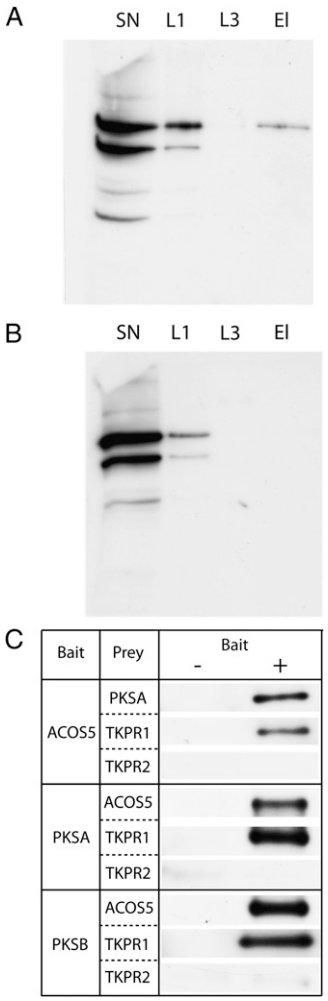

Figure 2. Protein-protein interactions evidenced by in vitro pull-down experiments. His-tagged bait protein and its potential prey were mixed with affinity beads, and after extensive washing the proteins were desorbed from nickel affinity beads with imidazole buffer. A, Assay with ACOS5 as bait and PKSA as prey; protein mixture (SN), washing solutions (L1 and L3), and eluted proteins (El) were immunoblotted using anti-PKSA serum; PKSA protein was found in proteins eluted from the affinity column. B, The assay was carried out as in A, except that no bait protein was added in protein mixture as control. No PKSA protein was detected after affinity column elution (El). C, The scheme summarizes the results obtained as shown in A and B; ACOS5, PKSA, and PKSB were tested as baits with PKSA, TKPR1, or TKPR2 as prey. Controls (–) were performed in the absence of bait. With varying baits, interactions were evidenced with ACOS5, PKSA, or TKPR1 as prey but never when TKPR2 was the prey.

acceptor. Since efficient energy transfer can only occur if distance between fluorophores is less than 10 nm, FRET can be used to monitor protein-protein interactions in living cells (Sun et al., 2012). To that aim, enhanced GFP (eGFP) was used as donor and fused to one protein of interest, and red fluorescent protein (RFP) was used as acceptor fused to a potential interactant. The change in the donor fluorescence lifetime in the presence of acceptor was measured by FLIM, and results are given in Figure 4. Controls were carried out with each donor in the presence of an ER marker that consisted of the amino acid sequence HDEL fused to RFP and used as acceptor. In the presence of PKSA and PKSB constructs, fluorescence lifetime value of ACOS5-eGFP was found significantly decreased compared with control (ACOS5/ER), as shown in Figure 4B, thus revealing interactions between ACOS5 and PKS proteins. A similar decrease of fluorescence lifetime was observed for the ACOS5 construct in the presence of TKPR1-RFP as acceptor. In contrast, the presence of TKPR2-RFP acceptor did not significantly affect ACOS5-eGFP donor fluorescence (Fig. 4B). Similarly Figure 4C shows that fluorescence lifetime of CYP704-eGFP donor is strongly decreased in the presence of PKSA-RFP, PKSB-RFP, and TKPR1-RFP constructs but not in the presence of TKPR2-RFP fusion, indicating efficient FRET in the former experiments but not in the latter. When PKSA-eGFP (Fig. 4D) or PKSB-eGFP (Fig. 4E) was used as donor, the most decreased lifetime value was monitored for homologous RFP constructs, thus confirming the formation of homodimers for both PKS proteins (Dobritsa et al., 2010). In contrast, the low level of FRET between PKSA and PKSB constructs indicates that PKS proteins do not associate in heteromers (Fig. 4, D and E). A strong decrease of lifetime of PKSA-eGFP and PKSB-eGFP was observed in the presence of TKPR1-RFP and ACOS5-RFP constructs, thus reflecting the interactions between PKS proteins and both TKPR1 and ACOS5. Low FRET level was monitored with TKPR2-RFP construct, confirming that TKPR2 is not closely associated with PKS proteins (Fig. 4, D and E).

Altogether, FLIM/FRET results indicate that ACOS5, PKSA, PKSB, TKPR1, and CYP704 proteins interact together on the endoplasmic reticulum of plant cells, whereas TKPR2 does not interact with either protein, in line with its distinct cytoplasmic localization (Fig. 1). Interactions between several enzymes of the pathway in planta suggest the occurrence of a sporopollenin metabolon that allows a rapid and efficient rate of biosynthesis of the exine building units by tapetal cells on pollen cell wall formation.

DISCUSSION

The exact structure of sporopollenin remains poorly understood because of a high level of resistance to chemical degradation. Genetic and molecular studies have recently demonstrated the role of fatty acid derivatives as general precursors of sporopollenin building units (Aarts et al., 1997; Morant et al., 2007; de Azevedo Souza et al., 2009; Dobritsa et al., 2009b; Grienenberger et al., 2010; Kim et al., 2010). Medium- and long-chain fatty acids are hydroxylated by CYP703 and CYP704 (Morant et al., 2007; Dobritsa et al., 2009b). Fatty acyl-CoA esters are synthesized by ACOS5 and condensed with malonyl-CoA by PKSA and PKSB to form tri- and tetraketide α-pyrones.

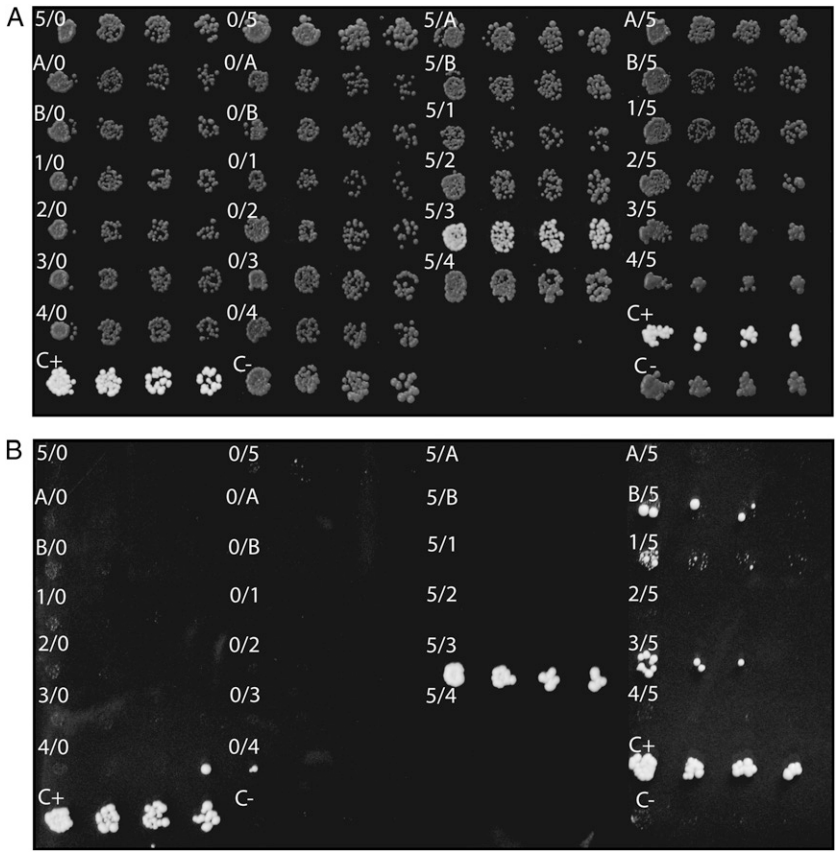

Figure 3. Protein-protein interactions shown by yeast two-hybrid analysis. Yeast cotransformed with varying couples of GAL4 AD and GAL4-DNA BD fused to sporopollenin biosynthetic enzymes was plated on selective medium at four dilutions. For each transformant, the first figure or letter indicates the protein fused to GAL4 AD and the second indicates the protein fused to GAL4 BD. The code is as follows: 5, ACOS5; A, PKSA; B, PKSB; 1, TKPR1; 2, TKPR2; 3, CYP703; CYP704; 0, empty plasmid. A, Yeast cotransformants were selected on medium lacking Leu and Trp. B, Selection of recombinant yeasts in the absence of His, Leu, and Trp. Growth demonstrates that interactions between enzymes of the sporopollenin pathway fused to GAL4 domains has induced *HIS* gene activation. Interactions were detected in the case of PKSB/ACOS5 (B/5 colonies), TKPR1/ACOS5 (1/5 colonies), ACOS5 and CYP703 (5/3 and 3/5 colonies). All controls transformed with either an empty AD or BD construct were negative (0/X or X/0), showing the absence of autoactivation in all cases. Maize (*Zea mays*) retinoblastoma protein (Rb1) and the RepA protein of wheat dwarf geminivirus served as positive controls (C+).

Tetraketides are then reduced by TKPR1 and TKPR2, giving rise to hydroxyl functions that are prone to form ether or ester linkages in the sporopollenin polymer.

In situ hybridization of mRNAs and immunolocalization of the cognate proteins have shown that sporopollenin biosynthetic genes are specifically expressed in anther tapetal cells (de Azevedo Souza et al., 2009; Grienenberger et al., 2010; Kim et al., 2010). Many ultrastructural features in line with an intense lipid metabolism have been reported in tapetal cells. For instance, ER dilation and accumulation of lipid-containing organelles named elaioplasts and tapetosomes have been observed in the tapetum at specific stages of anther development (Murgia et al., 1991; Owen and Makaroff, 1995; Piffanelli et al., 1997; Wu et al., 1997; Clément et al., 1998; Piffanelli et al., 1998; Hernández-Pinzón et al., 1999; Hsieh and Huang, 2005; Ishiguro et al., 2010). ER is known as an active center for lipid synthesis, and elaioplasts and tapetosomes have been shown to contain galactolipids, phospholipids, neutral esters, and triacylglycerides (Piffanelli et al., 1997; Hernández-Pinzón et al., 1999; Wu et al., 1997, 1999). Upon tapetal cell lysis, elaioplasts and tapetosomes are released in the anther locule, and the content of both organelles contributes to the formation of the lipidic coating of pollen grains. Concerning sporopollenin synthesis, our knowledge of the processes involved at the cellular level is fragmentary. For example, neither the sites of synthesis nor the mode of transfer of sporopollenin monomers from the tapetum into the locules prior to their polymerization into the microspore walls are known. Here we investigated the localization of the enzymes involved in the sporopollenin biosynthetic pathway, namely ACOS5, PKSA and PKSB, and TKPR1/2. Previously, translational fusions to GFP were transiently expressed in *N. benthamiana* leaves. For PKS and TKPR1 fusions but not for TKPR2 fusion, the fluorescence patterns indicated that the enzymes were associated to the ER of transgenic leaves (Grienenberger et al., 2010; Kim et al., 2010). Immunolocalization of the enzymes by TEM confirmed a preferred localization to ER for all the enzymes except TKPR2.

Multienzyme associations or metabolons have been reported for enzymes of primary and secondary metabolisms (Winkel-Shirley, 1999). Enzyme association affords high metabolic efficiency by allowing increased local substrate concentrations and by coordinating enzyme activities involved in the pathway. The occurrence of multienzyme complexes in phenylpropanoid and flavonoid pathways is believed to explain how common intermediates in these pathways may lead to distinct metabolites. Different experimental approaches such as radioactive labeling, cell fractionation, or microscopic studies have suggested

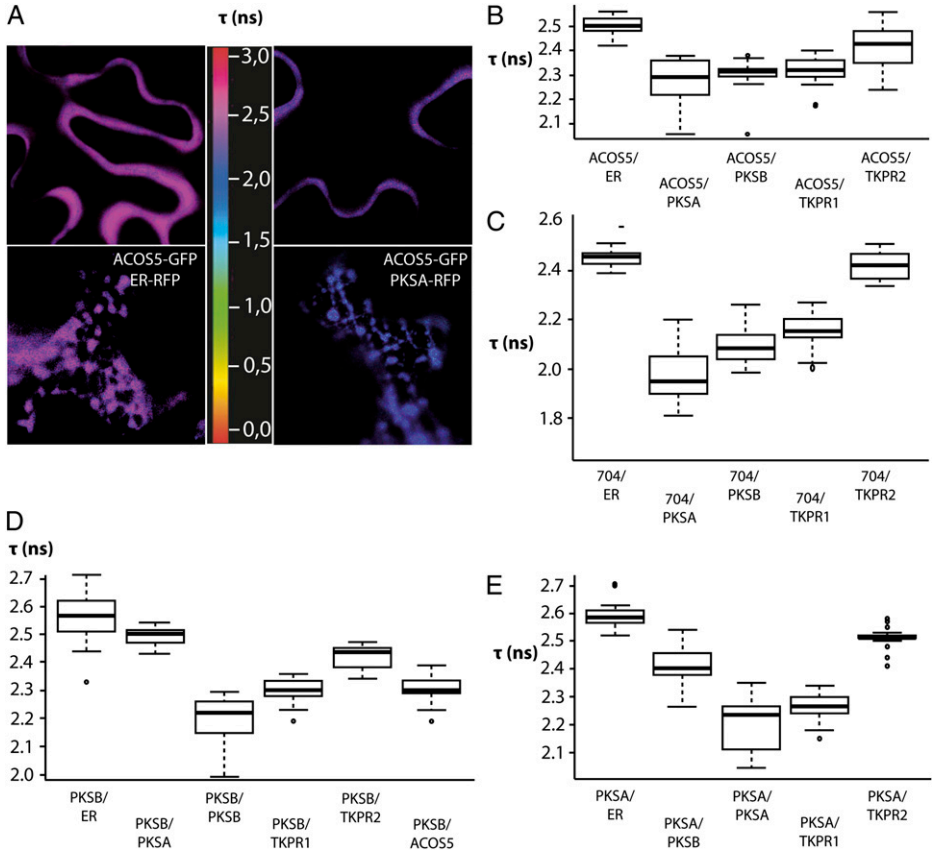

Figure 4. FLIM/FRET analysis demonstrates the interactions of sporopollenin enzymes in plant cells. A, Lifetime images of *N. benthamiana* leaves cotransformed with ACOS5-GFP and ER marker-RFP (control, left) or ACOS5-GFP and PKSA-RFP (right). Color indicates lifetime value as shown in the central scale. Images of whole cells are presented at the top, and at the bottom cortical sections show that changes in fluorescence lifetime localize mainly to the ER. B to E, Box plots (McGill et al., 1978) of lifetime values of different GFP fusions expressed in the presence of various RFP fusions. Each box includes 75% of a data set, with the bold line inside indicating the mean value and upper and lower bars marking the extreme values. B, ACOS5-GFP fluorescence lifetime measured in the presence of various protein-RFP constructs. Lifetime measured in the presence of an ER marker protein fused to RFP (ACOS5/ER marker) was taken as the control value. A decrease in fluorescence half-life was monitored in the presence of all RFP constructs except TKPR2 construct. These FLIM/FRET data revealed interactions of ACOS5 with PKSA, PKSB, and TKPR1 but not TKPR2. C, CYP704-GFP fluorescence half-life values in the presence of various RFP constructs. The pronounced decreases in fluorescence lifetime compared with control demonstrated interactions of CYP704 with PKSA, PKSB, and TKPR1 but not TKPR2. D, PKSB-GFP fluorescence lifetime after cotransformation with various RFP acceptors. Fluorescence lifetime was significantly decreased in the presence of PKSB-RFP construct, revealing the formation of homodimers. Markedly decreased lifetime values were also monitored in the presence ACOS5-RFP and TKPR1-RFP but not PKSA-RFP and TKPR2-RFP constructs. E, PKSA-GFP fluorescence half-life values in the presence of various RFP acceptors. The strongest decreases in fluorescence lifetime were monitored in the presence of PKSA-RFP and TKPR1-RFP constructs.

that enzyme complexes are structured on the ER, resulting in the channeling into a specific enzymatic reaction chain leading to a given final product (Czichi and Kindl, 1977; Hrazdina et al., 1987; Burbulis and Winkel-Shirley, 1999; Chen et al., 2011a). Distinct cytochrome P450 hydroxylases are involved in those pathways and serve as anchors of the metabolons to the ER membrane, as is likely the case for the sporopollenin metabolon evidenced in the present work. For example, a close association between Phe ammonia-lyase (PAL) and cinnamate 4-hydroxylase (C4H) that catalyze the two first steps of phenylpropanoid pathway, have been evidenced by measuring the relative incorporation of labeled Phe and cinnamic acid into *p*-coumaric acid, the direct C4H product: the higher rate of incorporation of labeled Phe suggested the occurrence of a metabolic channel arising from the interactions between PAL and C4H (Czichi and Kindl, 1977; Hrazdina and Wagner, 1985). Numerous experimental approaches have also indicated that enzymes of the flavonoid pathway interact to form complexes whose composition may vary, consequently leading to distinct end products (Hrazdina and Wagner, 1985; Burbulis and Winkel-Shirley, 1999; Winkel-Shirley, 1999). Recently, FLIM/FRET technology was used to demonstrate the direct interactions of chalcone synthase

with flavonol synthase or diflavonol reductase in living Arabidopsis protoplasts. These interactions are mutually exclusive, and their nature is thought to regulate the metabolic flux into the branch pathways (Crosby et al., 2011).

Here we provide evidence for the existence of a sporopollenin metabolon in anther tapetal cells. First, all tested enzymes (ACOS5, PKSA, PKSB, and TKPR1) but one (TKPR2) were preferentially localized to the ER of tapetal cells by immunoelectron microscopy (Fig. 1; Table I). Tagged recombinant proteins were shown to be pulled down in protein complexes that include various couples of bait and prey proteins (Fig. 2). These findings revealed the capacity of the enzymes involved in sporopollenin pathway to interact pairwise in vitro. It is noteworthy that TKPR2 was never found in protein complexes detected by pull-down experiments. Only a limited number of couples of proteins fused to an AD or BD allowed the reconstruction of functional GAL4 transcription factor in yeast two-hybrid system (Fig. 3) and thus confirmed the occurrence of protein-protein interactions in vivo for some combinations of proteins. When protein interactions were investigated in *N. benthanamia* cells by FLIM/FRET analysis, strong interactions were evidenced for all pairwise combinations of sporopollenin biosynthetic enzymes except those involving TKPR2 (Fig. 4). These results indicate that the enzymes ACOS5, PKSA, PKSB, and TKPR1 formed complexes associated to cytochromes P450. Cytochromes P450 are membrane proteins that are thought to serve as anchors to ER for associated proteins. This could be also the case for sporopollenin biosynthesis, but further evidence is needed to verify this assumption. On the other hand, interactions between enzymes that constitute a biosynthetic chain suggest that a metabolon may exist. The definitive demonstration would be required to show that the organization of enzymes into a metabolon results in a clear gain in term of catalysis efficiency.

The role of TKPR2 appears unclear. Genetic analysis has demonstrated its implication in pollen cell wall synthesis although the impact of TKPR2 mutation on exine formation appeared milder than that of the other sporopollenin biosynthetic genes and particularly that of the other reductase, TKPR1 (Grienenberger et al., 2010; Kim et al., 2010). Here, our results indicate that TKPR2 is not preferentially localized to the ER and is not strongly associated to other enzymes of the sporopollenin metabolon, even though a low FRET level could be detected in *N. benthanamia* in some cases (Fig. 4). This may indicate that a minor part of the protein is involved in sporopollenin biosynthesis, the function of the cytoplasmic fraction remaining unknown.

In tapetum, the existence of metabolon superstructures including the sporopollenin biosynthetic enzymes may explain the amazing efficiency of the pathway that catalyzes pollen cell wall building units during a short period of pollen development. Thus, intracellular organization of sporopollenin enzymes in metabolon may represent an additional level of regulation conferring efficiency, specificity, and plasticity to the biosynthetic pathway.

MATERIALS AND METHODS

Production of Recombinant Proteins and Specific Antibodies

Full coding sequences of At1g02050 (*PKSA*), At4g34850 (*PKSB*), At1g35420 (*TKPR1*), At1g68540 (*TKPR2*), and At1g62940 (*ACOS5*) genes were cloned in pGEX-KG after PCR amplification using forward and reverse primers as described in Kim et al. (2010). Error-free constructs were transformed into *Escherichia coli* BL21-G612 strain, a kanamycin-resistant strain that carries pLysS plasmid and expresses rare prokaryotic genes. Conditions of expression and purification of the recombinant proteins and procedures used for raising and purifying specific antibodies in rabbits were as previously described (Grienenberger et al., 2010; Kim et al., 2010).

TEM Immunolocalization

Flower buds expressing biosynthetic genes were selected as follows. On each inflorescence the ninth- to 11th-youngest buds were collected, counting backward from the bud having petals just protruding (stage 13, Smyth et al., 1990) as number one. Buds were fixed for 2 h with 3% (v/v) paraformaldehyde in 150 mM sodium phosphate buffer, pH 7.2, and postfixed in osmium tetraoxide. Samples were then stained with uranyl acetate and dehydrated in an ethanol gradient up to 100% (30 min each step) and then progressively embedded in LR white resin and allowed to polymerize for at least 48 h. Thin sections (70 nm) were taken using a diamond knife microtome (Reichert-Jung Ultracut E) and placed on formvar-coated nickel grids. Sections showing precise stage-8 to -9 anthers (Sanders et al., 1999) were identified by TEM and submitted to immunolabeling.

Before immunolabeling, sections were rehydrated in water and then blocked for 30 min in a phosphate-buffered saline (PBS) solution containing 1% bovine serum albumin. The rabbit antisera obtained and purified as described previously (Kim et al., 2010) were diluted 100- to 500-fold in the blocking solution. Thin sections were incubated in the serum solutions 2 h at room temperature. Then, after three successive washes with PBS buffer, sections were incubated for 2 h at room temperature with goat anti-rabbit igG coupled with 15-nm gold particles (Aurion, The Netherlands) diluted 1/50 in PBS containing 0.1% bovine serum albumin. Sections were then successively washed three times in PBS buffer and three times in water, then dried and observed using a Hitachi H-600 transmission electron microscope equipped with an Orca HR Hamamatsu camera.

Pull-Down Assays

The Arabidopsis At1g02050, At4g34850, At1g35420, and At1g62940 genes were cloned into the pHGWA and pGEX-KG vectors to be used as baits or prey, respectively. Constructs were transformed into *E. coli* SoluBL21 strain (AMS Biotechnology) to produce recombinant proteins. Prey proteins were purified as glutathione *S*-transferase fusions, and glutathione *S*-transferase tags were subsequently cleaved by thrombin. His-tagged bait proteins were purified on nickel agarose beads as described in the GE Healthcare HisTrap HP protocol. Purified proteins were eluted in 50 mM Tris-HCl buffer, pH 7.6, containing 15% (v/v) glycerol and EDTA-free complete miniprotease inhibitor cocktail (Roche).

For in vitro binding studies, 10 μg of bait and prey proteins were preincubated together for 1 h at 4°C in 300-μL buffer solution, pH 7.8, containing 20 mM MOPS, 500 mM NaCl, and 15% (v/v) glycerol. Then, 80 μL of His-select nickel affinity gel (Sigma) was added to the samples that were rotated for 1 h at 4°C. As control, each prey was incubated with the affinity gel in the absence of bait protein to evaluate nonspecific binding of the prey to the beads.

At the end of incubation, the samples were centrifuged at 4°C for 4 min at 1,000*g* and washed three times with 300 μL of 20 mM MOPS washing buffer, pH 7.8, containing 500 mM NaCl, 15% glycerol, and 20 mM imidazole. Proteins were eluted by incubation in 100 μL 20 mM MOPS buffer, pH 7.8, containing 500 mM NaCl, 15% glycerol, and 250 mM imidazole, and then separated by

12.5% SDS-PAGE and immunoblotted using a specific antiserum to detect the presence of the prey protein.

Yeast Two-Hybrid Assays

For two-hybrid analysis of interacting proteins, AH109 yeast (*Saccharomyces cerevisiae*) strain (Clontech) was used, and cotransformation was performed according to the Clontech yeast protocols handbook. The full-length open reading frames of At1g02050, At4g34850, At1g35420, At1g68540, At1g62940, At1g01280, and At1g69500 genes were amplified and inserted in frame with GAL4-BD in pGBKT7 vector or with the GAL4-AD domain in the pGADT7 vector (Clontech), under the control of 35S promoter in both cases. To test for autoactivation activity, the empty pGADT7 and one of the GAL4-BD fusions or the empty pGBKT7 and one of the GAL4-AD fusions were cotransformed into AH109 yeast cells and selected in the absence His, Leu, and Trp to check for autoactivation. The retinoblastoma protein (Rb1) of maize (*Zea mays*) and the RepA protein of wheat (*Triticum aestivum*) dwarf geminivirus were expressed and served as positive controls (Xie et al., 1996). No background activity was observed.

Cloning and Agroinfiltration of GFP or RFP Constructs

C-terminal fusions of the complementary DNAs encoding sporopollenin enzymes to eGFP or RFP were cloned by PCR using the primer pairs given in Supplemental Table S1. They were inserted under the control of CaMV 35S promoter into the expression vector pB7FWG2 or pB7RWG2, respectively, using the Gateway cloning system (Invitrogen). The monomeric RFP with the C-terminal amino acid extension HDEL served as ER marker. It was expressed under the control of a CaMV 35S promoter and a downstream signal sequence (Robinson et al., 2007). Constructs were transiently expressed in *Nicotiana benthamiana* leaves by agroinfiltration and imaged as described in Grienenberger et al. (2010).

FLIM

Three to 4 d after infiltration, fluorescent fusion protein lifetime was measured in the epidermal cells of infiltrated leaves for GFP constructs in the presence of various RFP constructs using a Nikon TE2000 microscope equipped with a 60×, 1.45-numerical aperture objective and a LIFA frequency domain fluorescence lifetime imaging system (Lambert Instruments). Measurements were acquired after excitation with a 483-nm light-emitting diode illumination source using a modulation frequency of 36 MHz and a fluorescein reference solution exhibiting a 4-ns lifetime. Two or three independent experiments have been performed and about 10 samples were analyzed in each experiment.

Supplemental Data

The following materials are available in the online version of this article.

Supplemental Table S1. Primers used for cloning.

ACKNOWLEDGMENTS

We thank Drs. C. Ritzenthaler and J. Mutterer for help with confocal microscopy and FLIM/FRET measurements, and Dr. J.-M. Davière for help and advice regarding two-hybrid assays.

Received December 21, 2012; accepted April 19, 2013; published April 30, 2013.

LITERATURE CITED

Aarts MG, Hodge R, Kalantidis K, Florack D, Wilson ZA, Mulligan BJ, Stiekema WJ, Scott R, Pereira A (1997) The Arabidopsis MALE STERILITY 2 protein shares similarity with reductases in elongation/condensation complexes. Plant J **12:** 615–623

Ahlers F, Lambert J, Wiermann R (2003) Acetylation and silylation of piperidine solubilized sporopollenin from pollen of Typha angustifolia L. Z Naturforsch C **58:** 807–811

Ariizumi T, Toriyama K (2011) Genetic regulation of sporopollenin synthesis and pollen exine development. Annu Rev Plant Biol **62:** 437–460

Blackmore S, Wortley AH, Skvarla JJ, Rowley JR (2007) Pollen wall development in flowering plants. New Phytol **174:** 483–498

Bubert H, Lambert J, Steuernagel S, Ahlers F, Wiermann R (2002) Continuous decomposition of sporopollenin from pollen of Typha angustifolia L. by acidic methanolysis. Z Naturforsch C **57:** 1035–1041

Burbulis IE, Winkel-Shirley B (1999) Interactions among enzymes of the Arabidopsis flavonoid biosynthetic pathway. Proc Natl Acad Sci USA **96:** 12929–12934

Chen HC, Li Q, Shuford CM, Liu J, Muddiman DC, Sederoff RR, Chiang VL (2011a) Membrane protein complexes catalyze both 4- and 3-hydroxylation of cinnamic acid derivatives in monolignol biosynthesis. Proc Natl Acad Sci USA **108:** 21253–21258

Chen W, Yu XH, Zhang K, Shi J, De Oliveira S, Schreiber L, Shanklin J, Zhang D (2011b) Male Sterile2 encodes a plastid-localized fatty acyl carrier protein reductase required for pollen exine development in Arabidopsis. Plant Physiol **157:** 842–853

Choi H, Jin JY, Choi S, Hwang JU, Kim YY, Suh MC, Lee Y (2011) An ABCG/WBC-type ABC transporter is essential for transport of sporopollenin precursors for exine formation in developing pollen. Plant J **65:** 181–193

Clément C, Laporte P, Audran JC (1998) The loculus content and tapetum during pollen development in *Lilium.* Sex Plant Reprod **11:** 94–106

Crosby KC, Pietraszewska-Bogiel A, Gadella TWJ Jr, Winkel BS (2011) Förster resonance energy transfer demonstrates a flavonoid metabolon in living plant cells that displays competitive interactions between enzymes. FEBS Lett **585:** 2193–2198

Czichi U, Kindl H (1977) Phenylalanine ammonia-lyase and cinnamic acid hydroxylases as assembled consecutive enzymes on microsomal-membranes of cucumber cotyledons: Cooperation and subcellular-distribution. Planta **134:** 133–143

de Azevedo Souza C, Kim SS, Koch S, Kienow L, Schneider K, McKim SM, Haughn GW, Kombrink E, Douglas CJ (2009) A novel fatty Acyl-CoA Synthetase is required for pollen development and sporopollenin biosynthesis in *Arabidopsis*. Plant Cell **21:** 507–525

Dobritsa AA, Geanconteri A, Shrestha J, Carlson A, Kooyers N, Coerper D, Urbanczyk-Wochniak E, Bench BJ, Sumner LW, Swanson R, et al (2011) A large-scale genetic screen in Arabidopsis to identify genes involved in pollen exine production. Plant Physiol **157:** 947–970

Dobritsa AA, Lei Z, Nishikawa S, Urbanczyk-Wochniak E, Huhman DV, Preuss D, Sumner LW (2010) LAP5 and LAP6 encode anther-specific proteins with similarity to chalcone synthase essential for pollen exine development in Arabidopsis. Plant Physiol **153:** 937–955

Dobritsa AA, Nishikawa S-I, Preuss D, Urbanczyk-Wochniak E, Sumner LW, Hammond A, Carlson AL, Swanson RJ (2009a) *LAP3,* a novel plant protein required for pollen development, is essential for proper exine formation. Sex Plant Reprod **22:** 167–177

Dobritsa AA, Shrestha J, Morant M, Pinot F, Matsuno M, Swanson R, Møller BL, Preuss D (2009b) CYP704B1 is a long-chain fatty acid ω-hydroxylase essential for sporopollenin synthesis in pollen of Arabidopsis. Plant Physiol **151:** 574–589

Dominguez E, Mercado JA, Quesada MA, Heredia A (1999) Pollen sporopollenin: degradation and structural elucidation. Sex Plant Reprod **12:** 171–178

Dou XY, Yang KZ, Zhang Y, Wang W, Liu XL, Chen LQ, Zhang XQ, Ye D (2011) WBC27, an adenosine tri-phosphate-binding cassette protein, controls pollen wall formation and patterning in Arabidopsis. J Integr Plant Biol **53:** 74–88

Grienenberger E, Kim SS, Lallemand B, Geoffroy P, Heintz D, Souza CdeA, Heitz T, Douglas CJ, Legrand M (2010) Analysis of *TETRAKETIDE α-PYRONE REDUCTASE* function in *Arabidopsis thaliana* reveals a previously unknown, but conserved, biochemical pathway in sporopollenin monomer biosynthesis. Plant Cell **22:** 4067–4083

Hernández-Pinzón I, Ross JH, Barnes KA, Damant AP, Murphy DJ (1999) Composition and role of tapetal lipid bodies in the biogenesis of the pollen coat of Brassica napus. Planta **208:** 588–598

Hrazdina G, Wagner GJ (1985) Metabolic pathways as enzyme complexes: evidence for the synthesis of phenylpropanoids and flavonoids on membrane associated enzyme complexes. Arch Biochem Biophys **237:** 88–100

Hrazdina G, Zobel AM, Hoch HC (1987) Biochemical, immunological, and immunocytochemical evidence for the association of chalcone synthase

with endoplasmic reticulum membranes. Proc Natl Acad Sci USA **84:** 8966–8970

Hsieh K, Huang AH (2005) Lipid-rich tapetosomes in Brassica tapetum are composed of oleosin-coated oil droplets and vesicles, both assembled in and then detached from the endoplasmic reticulum. Plant J **43:** 889–899

Hsieh K, Huang AH (2007) Tapetosomes in *Brassica tapetum* accumulate endoplasmic reticulum-derived flavonoids and alkanes for delivery to the pollen surface. Plant Cell **19:** 582–596

Huang MD, Wei FJ, Wu CC, Hsing YI, Huang AH (2009) Analyses of advanced rice anther transcriptomes reveal global tapetum secretory functions and potential proteins for lipid exine formation. Plant Physiol **149:** 694–707

Ishiguro S, Nishimori Y, Yamada M, Saito H, Suzuki T, Nakagawa T, Miyake H, Okada K, Nakamura K (2010) The Arabidopsis FLAKY POLLEN1 gene encodes a 3-hydroxy-3-methylglutaryl-coenzyme A synthase required for development of tapetum-specific organelles and fertility of pollen grains. Plant Cell Physiol **51:** 896–911

Kim SS, Grienenberger E, Lallemand B, Colpitts CC, Kim SY, Souza CdeA, Geoffroy P, Heintz D, Krahn D, Kaiser M, et al (2010) *LAP6/POLYKETIDE SYNTHASE A* and *LAP5/POLYKETIDE SYNTHASE B* encode hydroxyalkyl α-pyrone synthases required for pollen development and sporopollenin biosynthesis in *Arabidopsis thaliana*. Plant Cell **22:** 4045–4066

McGill R, Tukey JW, Larsen WA (1978) Variations of box plots. Am Stat **32:** 12–16

Mizuuchi Y, Shimokawa Y, Wanibuchi K, Noguchi H, Abe I (2008) Structure function analysis of novel type III polyketide synthases from Arabidopsis thaliana. Biol Pharm Bull **31:** 2205–2210

Morant M, Jørgensen K, Schaller H, Pinot F, Møller BL, Werck-Reichhart D, Bak S (2007) CYP703 is an ancient cytochrome P450 in land plants catalyzing in-chain hydroxylation of lauric acid to provide building blocks for sporopollenin synthesis in pollen. Plant Cell **19:** 1473–1487

Murgia M, Charzynska M, Rougier M, Cresti M (1991) Secretory tapetum of *Brassica oleracea* L.: polarity and ultrastructural features. Sex Plant Reprod **4:** 28–35

Owen HA, Makaroff CA (1995) Ultrastructure of microsporogenesis and microgametogenesis in *Arabidopsis thaliana* (L.) Heynh. ecotype Wassilewskija (Brassicaceae). Protoplasma **185:** 7–21

Paxson-Sowders DM, Dodrill CH, Owen HA, Makaroff CA (2001) DEX1, a novel plant protein, is required for exine pattern formation during pollen development in Arabidopsis. Plant Physiol **127:** 1739–1749

Piffanelli P, Ross JH, Murphy DJ (1997) Intra- and extracellular lipid composition and associated gene expression patterns during pollen development in Brassica napus. Plant J **11:** 549–562

Piffanelli P, Ross JHE, Murphy DJ (1998) Biogenesis and function of the lipidic structures of pollen grains. Sex Plant Reprod **11:** 65–80

Quilichini TD, Friedmann MC, Samuels AL, Douglas CJ (2010) ATP-binding cassette transporter G26 is required for male fertility and pollen exine formation in Arabidopsis. Plant Physiol **154:** 678–690

Robinson DG, Herranz M-C, Bubeck J, Pepperkok R, Ritzenthaler C (2007) Membrane dynamics in the early secretory pathway. Crit Rev Plant Sci **26:** 199–225

Sanders PM, Bui AQ, Weterings K, McIntire KN, Hsu Y-C, Lee PY, Truong MT, Beals TP, Goldberg RB (1999) Anther developmental defects in *Arabidopsis thaliana* male-sterile mutants. Sex Plant Reprod **11:** 297–322

Scott RJ, Spielman M, Dickinson HG (2004) Stamen structure and function. Plant Cell **16**(Suppl): S46–S60

Smyth DR, Bowman JL, Meyerowitz EM (1990) Early flower development in *Arabidopsis*. Plant Cell **2:** 755–767

Sun Y, Hays NM, Periasamy A, Davidson MW, Day RN (2012) Monitoring protein interactions in living cells with fluorescence lifetime imaging microscopy. Methods Enzymol **504:** 371–391

Suzuki T, Masaoka K, Nishi M, Nakamura K, Ishiguro S (2008) Identification of kaonashi mutants showing abnormal pollen exine structure in Arabidopsis thaliana. Plant Cell Physiol **49:** 1465–1477

Tang LK, Chu H, Yip WK, Yeung EC, Lo C (2009) An anther-specific dihydroflavonol 4-reductase-like gene (DRL1) is essential for male fertility in Arabidopsis. New Phytol **181:** 576–587

Winkel-Shirley B (1999) Evidence for enzyme complexes in the phenylpropanoid and flavonoid pathways. Physiol Plant **107:** 142–149

Wu SS, Moreau RA, Whitaker BD, Huang AH (1999) Steryl esters in the elaioplasts of the tapetum in developing Brassica anthers and their recovery on the pollen surface. Lipids **34:** 517–523

Wu SS, Platt KA, Ratnayake C, Wang TW, Ting JT, Huang AH (1997) Isolation and characterization of neutral-lipid-containing organelles and globuli-filled plastids from Brassica napus tapetum. Proc Natl Acad Sci USA **94:** 12711–12716

Xie Q, Sanz-Burgos AP, Hannon GJ, Gutiérrez C (1996) Plant cells contain a novel member of the retinoblastoma family of growth regulatory proteins. EMBO J **15:** 4900–4908

Zhang D, Liang W, Yin C, Zong J, Gu F, Zhang D (2010) OsC6, encoding a lipid transfer protein, is required for postmeiotic anther development in rice. Plant Physiol **154:** 149–162

Zheng Z, Xia Q, Dauk M, Shen W, Selvaraj G, Zou J (2003) Arabidopsis *AtGPAT1*, a member of the membrane-bound glycerol-3-phosphate acyltransferase gene family, is essential for tapetum differentiation and male fertility. Plant Cell **15:** 1872–1887